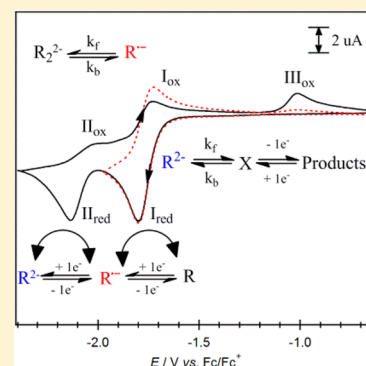


Competing Hydrogen-Bonding, Decomposition, and Reversible Dimerization Mechanisms during the One- and Two-Electron Electrochemical Reduction of Retinal (Vitamin A)

Ying Shan Tan, Yanni Yue, and Richard D. Webster*

Division of Chemistry and Biological Chemistry, School of Physical and Mathematical Sciences, Nanyang Technological University, Singapore 637371, Singapore

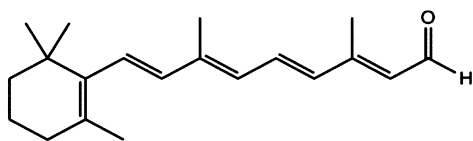
ABSTRACT: Retinal (R) can be sequentially voltammetrically reduced in CH₃CN in two one-electron processes to form first the anion radical (R^{•-}) at -1.75 (±0.04) V vs Fc/Fc⁺ (Fc = ferrocene) then the dianion (R²⁻) at -2.15 (±0.04) V vs Fc/Fc⁺. The anion radical undergoes a reversible dimerization reaction to form the dianion (R₂²⁻) with a forward dimerization rate constant $k_{\text{dim}} = 8 \times 10^2 \text{ L mol}^{-1} \text{ s}^{-1}$ and a reverse monomerization rate constant $k_{\text{mon}} = 2 \times 10^{-2} \text{ s}^{-1}$ at 295 K. All three anion species (anion radical, dianion, and dimer dianion) undergo hydrogen-bonding interactions with water that is present at millimolar levels in the solvent. As the water content of the solvent increases, the fate of the reduced compounds is determined by chemically irreversible hydrolysis reactions with H₂O and decomposition reactions of the highly charged R²⁻. Bulk-controlled potential electrolysis experiments combined with NMR analysis of the reaction solutions indicate that the reduction occurs at the aldehyde group of retinal. The electrochemical data obtained under a range of experimental conditions (varying voltammetric scan rates, temperatures, H₂O content of solutions, and retinal concentrations) were modeled by digital simulation techniques to determine the kinetic and thermodynamic parameters associated with all of the homogeneous reactions.



1. INTRODUCTION

Retinal is a form of vitamin A found in plants and is thought to be the product of the oxidative cleavage of β -carotene (Scheme 1).^{1–3} Being a liposoluble vitamin, retinal is stored in fat cells in

Scheme 1. Structure of All-trans Retinal



the body, where it can also undergo various chemical conversion processes.^{4–7} In physiological reactions, retinal is recognized as being used as a visual pigment in the eye in order to enhance night vision.⁸ It is possible for retinal to chemically convert to other forms of vitamin A, such as retinol and retinoic acid, depending on certain key biochemical reactions within the body. Retinal is also thought to be beneficial as an antioxidant⁵ and to have preventive effects for various diseases and cancers.^{6–10}

As retinal exists in epithelial cells in the skin, it helps to prevent skin diseases by acting as a first line of defense. Because the transformations between the different forms of vitamin A can involve oxidation or reduction mechanisms inside lipophilic membranes, it is interesting to examine the voltammetric properties of the compound in a low-water environment.

Several detailed studies have been performed on electrochemical reaction mechanisms related to carotenoid com-

pounds,^{11–13} which have molecular structures similar to retinal. Despite the fact that retinal is a common and beneficial form of vitamin A, little is known of the exact electrochemical reaction mechanism it undergoes. It has been proposed that retinal undergoes an initial one-electron reduction to generate an anion radical.^{14,15} The homogeneous reactions following the generation of the anion radical have led to some uncertainty as to whether a dimerization process or a hydrolysis reaction with trace water in the solvent (or both processes) takes place. Previous studies have tried to decipher whether a protonation reaction or dimerization reaction takes place by using various methods such as electrochemical kinetic studies,¹³ theoretical calculations,¹⁴ and spectroscopic experiments.^{14,15} Some studies have also proposed a disproportionation step in which the doubly reduced retinal (a dianion) reacts with the starting material to form two molecules of the anion radical.¹⁴ The actual site of the molecule undergoing reduction is still unclear as it could possibly occur within the polyene chain or at the carbonyl group.¹⁶ Electrochemical reduction experiments have been performed on activated olefins, and it has been shown that they undergo dimerization through their associated anion radicals.^{17–20} In alkaline ethanol solutions, benzaldehyde undergoes reductive dimerization through its radical anion.^{21,22} It has been proposed that reduced retinal undergoes

Received: May 26, 2013

Revised: July 12, 2013

Published: July 23, 2013

dimerization when proton donors are present, similar to malonate esters.^{23,24}

In this study we have used variable scan rate cyclic voltammetry combined with digital simulation modeling of the data to better understand the reduction mechanism of retinal. The focus was on determining whether the reduced species underwent hydrogen-bonding interactions with water, hydrolysis (protonation reactions), or whether the simulations supported a dimerization reaction of the anion radicals.

2. EXPERIMENTAL SECTION

2.1. Chemicals. All-*trans* retinal ($\geq 98\%$) was obtained from Sigma-Aldrich and stored in the dark at 277 K. Bu_4NPF_6 was prepared by reacting equimolar amounts of aqueous solutions of Bu_4NOH (40%, Alfa Aesar) and HPF_6 (65%, Fluka), washing the precipitate with hot water, and recrystallizing three times from hot ethanol. The sample was then dried under vacuum at 433 K for 6 h and stored under vacuum. Molecular sieves in the form $1/16$ in. rods with 3 Å pore size (CAS 308080-99-1) were obtained from Fluka. Acetonitrile was either high-performance liquid chromatography or analytical grade and used directly from bottles (after drying over 3 Å molecular sieves) unless otherwise stated. Purified water, with a resistivity $\geq 18 \text{ M}\Omega \text{ cm}$, was obtained from an ELGA Purelab Option-Q system.

2.2. Voltammetry. Cyclic voltammetry (CV) experiments were conducted with a computer-controlled Metrohm Autolab PGSTAT302N potentiostat. The working electrode was a 1 mm diameter glassy carbon (GC) disk (Cypress Systems) and was used in conjunction with a Pt auxiliary electrode (Metrohm) and a Ag wire miniature reference electrode (Cypress Systems) connected to the test solution via a salt bridge containing 0.5 M Bu_4NPF_6 in CH_3CN . The internal filling solution of the reference electrode was prepared immediately prior to use to reduce contamination from water in the reference electrode filling solution. Accurate potentials were obtained using ferrocene as an internal standard. Digital simulations of the CV data were performed using the DigiElch software package.^{25–30} Variable-temperature experiments were performed in a Metrohm jacketed glass cell with the temperature controlled with a Julabo FP89-HL ultralow refrigerated circulator.

Controlled potential electrolysis with coulometry was performed in a two-compartment cell using Pt mesh baskets as the working and auxiliary electrodes and with the Ag wire miniature reference electrode placed in the working electrode compartment solution. The volumes of the working and auxiliary electrode compartments were approximately 20 mL, and both solutions were continually purged with a stream of Ar gas to simultaneously stir the solutions and maintain an inert atmosphere.

2.3. Measurement of Water Content of Organic Solvents. The drying process was carried out on the solvent and electrolyte prior to the start of the experiment. CH_3CN was first dried using molecular sieves. The sieves were heated to 413 K for 6 h, added to the solvent in the solvent bottle, and left to stand for 24 h with occasional swirling to facilitate the drying process. A 0.2 M supporting electrolyte was weighed into a 25 mL volumetric flask and heated to 413 K for 6 h in a vacuum oven. After the electrolyte was heated, it was dissolved with 25 mL of dried solvent from the solvent bottle. The solvent/electrolyte mixture was poured into the predried vacuum syringe (containing molecular sieves) and kept under a

constant flow of nitrogen gas for 2 days before being used. A sample of $2 \times 10^{-3} \text{ M}$ retinal was weighed, added to the electrochemical cell, and dissolved with 5 mL of the dried solvent/electrolyte mixture from the syringe. A control electrochemical cell containing just the solvent/electrolyte was used to estimate the amount of water entering the electrochemical cell over time under natural humidity conditions.

Karl Fischer (KF) titrations were conducted with a Mettler Toledo DL32 coulometer using (Riedel-deHaën) HYDRANAL-Coulomat CG for the cathode compartment and HYDRANYL-Coulomat AG for the anode compartment. The chemicals were all obtained from Sigma-Aldrich. The water content of the solvent/electrolyte mixture under dry experimental conditions was estimated by KF titrations to be $\sim 20 \times 10^{-3} \text{ M}$ in the electrochemical cell. Constant humidity measurements were conducted in a ($122 \times 61 \times 61 \text{ cm}^3$) humidity control glovebox using a dry nitrogen purge system from Coy Laboratory Products Inc.³¹

3. RESULTS AND DISCUSSION

3.1. Cyclic Voltammetry of Retinal in Acetonitrile with Low Water Concentrations. CH_3CN was used in this study because it is less hygroscopic than other aprotic solvents suitable for electrochemistry, such as dimethyl sulfoxide and dimethylformamide, enabling the initial water content to be more easily maintained at a relatively low level.³¹ While chlorinated solvents such as dichloromethane and 1,2-dichloroethane are less hygroscopic than CH_3CN , they have a limited reductive potential range that makes it difficult to detect all of the voltammetric processes of retinal.

Voltammograms of retinal in CH_3CN containing 0.2 M Bu_4NPF_6 at room temperature ($295 \pm 2 \text{ K}$) show two reduction processes at negative potentials (solid black line in Figure 1a, peaks I_{red} and II_{red}). Bulk-controlled potential electrolysis (with coulometry) was conducted to find the

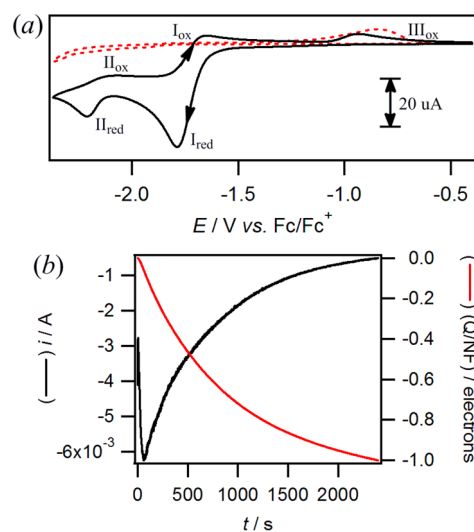


Figure 1. (a) CV data of $2 \times 10^{-2} \text{ M}$ retinal in CH_3CN ($[\text{H}_2\text{O}] = 50 (\pm 10) \text{ mM}$) containing 0.2 M Bu_4NPF_6 at $295 \pm 2 \text{ K}$ obtained at a 1 mm GC electrode at a scan rate of 0.1 V s^{-1} ; (solid black line) before and (dotted red line) after the transfer of one electron per molecule in a controlled potential electrolysis cell. (b) Current and coulometry versus time data obtained during the reductive electrolysis of retinal at $-1.9 \text{ V vs Fc/Fc}^+$.

number of electrons transferred in the first reduction process (Figure 1b). The coulometry experiments indicated that the first reduction peak was a one-electron process, which resulted in the formation of the radical anion $R^{\bullet-}$.

At a scan rate of 100 mV s^{-1} , both the first and second reduction processes display much smaller reverse oxidative peak currents (i_p^{ox}) compared to their forward reductive peak currents (i_p^{red}) ($i_p^{\text{ox}}/i_p^{\text{red}} \ll 1$), which is due to chemical instability of the reduced compounds (Figure 2). An oxidation

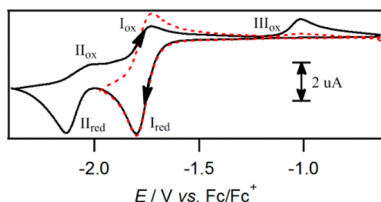


Figure 2. CV data of $2 \times 10^{-3} \text{ M}$ retinal in CH_3CN ($[\text{H}_2\text{O}] = 50 (\pm 10) \text{ mM}$) containing 0.2 M Bu_4NPF_6 at $295 \pm 2 \text{ K}$ obtained at a 1 mm GC working electrode at a scan rate of 0.1 V s^{-1} .

peak (III_{ox}) appears at a potential of approximately -1.0 V vs Fc/Fc^+ only if the scan is first applied in the negative potential direction past the first one-electron reduction process and is thus associated with the oxidation of a secondary product of the reduction. Multiple scans showed no reverse (reduction) peak for process III_{ox} indicating that the generated product is itself short-lived when it is oxidized. It is possible that other secondary products have also been formed after the reduction processes and are not redox active or do not fall within the potential window of CH_3CN (using a GC electrode).

When the scan direction is reversed after the second reduction process at approximately -2.2 V vs Fc/Fc^+ , two small oxidation processes are detected (I_{ox} and II_{ox}), which are the reverse processes of I_{red} and II_{red} , respectively. The first reduction process (I_{red}) is due to the formation of the radical anion, and the second reduction process (II_{red}) is the further one-electron reduction of the radical anion to form the dianion (R^{2-}). At slow scan rates ($< 10 \text{ V s}^{-1}$), the i_p^{red} value for the second process is smaller than the i_p^{red} value for the first process because the radical anion is undergoing other homogeneous reactions before it has time to be reduced to the dianion. Halting the forward potential scan just after the first electron transfer process (Figure 2) resulted in an increase in the size of the i_p^{ox} value for process I_{ox} because there were more radical anions at the electrode surface able to undergo oxidation back to the starting material. However, the subsequent oxidation peak at approximately -1.0 V vs Fc/Fc^+ becomes much smaller, suggesting that the species responsible for this process are formed in a higher amount after the second reduction step. Another possible explanation is that process III_{ox} is associated with the oxidation of multiple species formed from homogeneous reactions of $\text{R}^{\bullet-}$ and R^{2-} that are coincidentally oxidized at similar potentials. Experiments were also conducted by scanning values more negative than the second reduction peak potential; however, there was no obvious reduction process following the second reduction.

Background voltammograms of just the solvent and electrolyte were performed at all scan rates to reduce contributions from the charging current and minor solvent impurities detected with the use of the 1 mm diameter GC working electrode. All CV data are presented minus their backgrounds to more clearly show the retinal peaks under the reaction

conditions stated. CV data of $2 \times 10^{-3} \text{ M}$ retinal in CH_3CN containing 0.2 M Bu_4NPF_6 recorded at 1 mm diameter GC working electrode at variable scan rates show that as the scan rate increases, the first reduction peak becomes more chemically reversible (Figure 3). The oxidation peak (III_{ox}) at

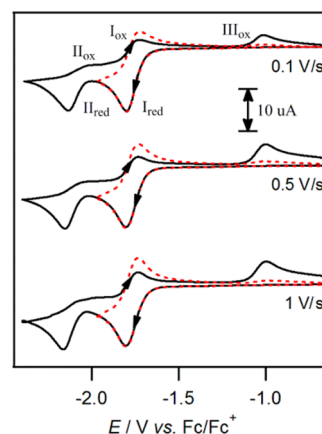


Figure 3. CV data of $2 \times 10^{-3} \text{ M}$ retinal in CH_3CN ($[\text{H}_2\text{O}] = 50 (\pm 10) \text{ mM}$) containing 0.2 M Bu_4NPF_6 at $295 \pm 2 \text{ K}$ obtained at a 1 mm GC working electrode at variable scan rates (ν) of $0.1, 0.5,$ and 1.0 V s^{-1} . The current axis has been scaled by multiplying by $\nu^{-0.5}$.

approximately -1.0 V vs Fc/Fc^+ displays a large difference in peak current depending on whether the scan direction is switched immediately after the first or second reduction process. It appears that the species responsible for process III_{ox} are produced from both the first and second one-electron reduction steps, but a larger proportion of the product comes after the generation of the dianion.

Variable scan rate experiments were also conducted at several different temperatures: $295, 283, 273, 263, 253,$ and 243 K (Figure 4). It was found that the chemical reversibility of the first and second electron transfer steps did not change substantially with changing temperature, indicating that the lifetime of the dianion did not noticeably improve at low temperatures. Even at a scan rate of 20 V s^{-1} , the reverse oxidation peak (II_{ox}) remains very small. The peak currents of the reduction and oxidation processes decreased as the temperature was lowered because of slower diffusion rates of the species involved. Some interesting changes with temperature were observed for process III_{ox} . As Figure 4a shows, the oxidation process III_{ox} which occurs at approximately -1.0 V vs Fc/Fc^+ at 295 K , shifts more positively to approximately -0.9 V vs Fc/Fc^+ at 243 K . The peak also changes from a sharp peak at higher temperatures to a flattened peak at lower temperatures, possibly because of the separation into two electron transfer processes. Examination of Figure 4b, in which the potential was switched just after the first electron transfer step, reveals that the small oxidation peak at approximately -1.0 V vs Fc/Fc^+ also shifted more positively with decreasing temperatures. The III_{ox} process in the right column is always at a potential that is slightly more positive than that of the III_{ox} process in the left column where the switching potential is more negative. This indicates that it is possible that different secondary products (but with similar oxidation potentials) were generated depending on whether the scan direction is switched just after the first or second electron transfer reduction process. Therefore, different reaction pathways exist for the radical

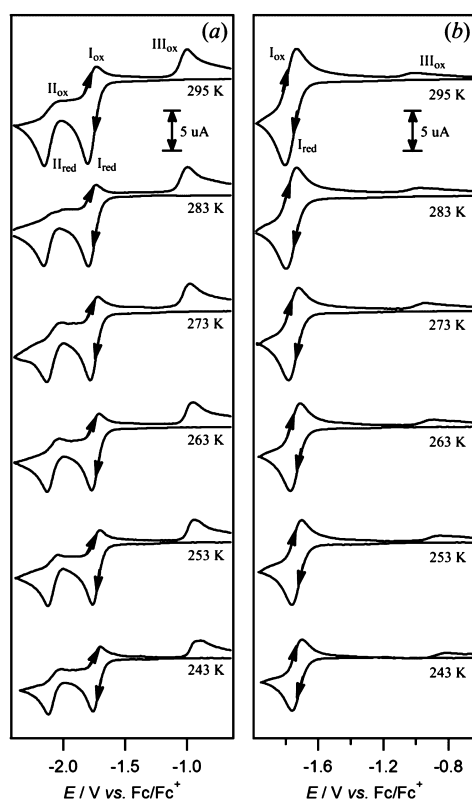


Figure 4. CV data of 2×10^{-3} M retinal in CH_3CN ($[\text{H}_2\text{O}] = 50\text{--}100$ mM) containing 0.2 M Bu_4NPF_6 at variable temperatures recorded at a 1 mm GC working electrode at a scan rate of 0.5 V s^{-1} .

anion and dianion generated after the initial heterogeneous electron transfer reduction steps.

Experiments with 1×10^{-3} , 2×10^{-3} , and 5×10^{-3} M retinal were performed in order to assess concentration effects on the voltammetric reduction mechanism (Figure 5). As the concentration increased, the second reduction peak decreased in size relative to the first reduction process, showing that with increasing concentration of retinal, fewer radical anions are able to undergo further reduction to the dianion. Furthermore, as the concentration of retinal increased, the chemical reversibility of the first reduction process appeared to decrease. These results provide evidence of a dimerization process after the formation of the radical anion (eq 1).



The change in peak current ratios can also be seen clearly in Figure 1 in which a very high 20 mM concentration of retinal shows a second reduction process (II_{red}) that is much smaller than the first process (I_{red}) at a scan rate of 0.1 V s^{-1} . When the radical anion is generated after the first reduction step, two molecules can react together and dimerize, resulting in fewer radical anions being reduced in the second reduction process. With a greater concentration of starting material, it is more likely that the radical anions can react; hence, more dimerized product will be formed. This can also be voltammetrically observed by looking at Figure 5b, where a greater concentration of retinal (5×10^{-3} M) gives a less chemically reversible first reduction peak compared to that of lower concentrations, showing that more of the radical anions had dimerized. It can be observed in the voltammograms in Figure 5b that the oxidation peak at approximately -1.0 V vs Fc/Fc^+ (III_{ox})

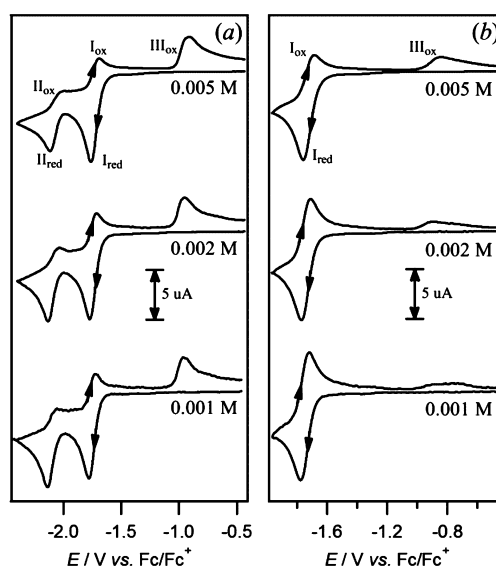


Figure 5. CV data of 1×10^{-3} , 2×10^{-3} , and 5×10^{-3} M retinal in CH_3CN ($[\text{H}_2\text{O}] = 60 (\pm 10)$ mM) containing 0.2 M Bu_4NPF_6 at 263 K obtained at a 1 mm GC working electrode at a scan rate of 0.5 V s^{-1} with different switching potentials. The current scale has been normalized (to 0.002 M retinal) so that the first reduction process appears to be the same size in each voltammogram.

appears relatively larger (compared to the oxidation peak I_{ox}) at high concentrations compared to that at a low concentration. This suggests that process III_{ox} , which is evident when the scan is reversed just after the first one-electron reduction, can be assigned to the oxidation of the newly formed dimerized species. The peak height registered at lower concentration is smaller because less dimerized product is formed. This in turn gives a more chemically reversible peak for the first reduction process at lower concentrations. There are several reports of the radical anions of aromatic compounds produced by electrochemical methods undergoing reversible dimerization reactions.^{32–38} The dimers of the radical anions have been reported to be more difficult to oxidize than the radical anions, which results in cyclic voltammograms showing an oxidation process a few hundred mV more positive than the oxidation of the radical anion (i.e., consistent with process III_{ox}).

Synthetic scale-controlled potential electrolysis experiments were performed by electrolyzing 140 mg of retinal. Thin-layer chromatography analysis of the reaction mixture at the completion of the electrolysis showed a number of products that were not easily separated and purified by preparative column chromatography. Nevertheless, ^{13}C NMR spectroscopy performed on the entire reaction mixture showed no carbonyl carbon resonance, indicating that the aldehyde group had undergone reduction. Similarly, Fourier transform infrared analysis of the reaction mixture did not lead to the detection of a carbonyl stretching band. Therefore, it is possible that the dimerization occurs through the carbonyl group to form a pinacol, as has been previously proposed.²³ However, we were not able to obtain spectroscopic evidence for the existence of the dimer on the synthetic time scale; thus, it is equally probable that the dimer exists only as an intermediate in solution, which is often the case in reversible dimerization reactions.^{32–38} Furthermore, because of the relatively high reduction potential, it is unlikely that dianionic dimers would survive as intermediates under the conditions used for liquid

chromatography–mass spectrometry or gas chromatography–mass spectrometry experiments.

The experiments conducted with varying temperature, scan rate, and concentration help identify the likely reduction mechanism that retinal undergoes, which is consistent with a radical dimerization mechanism (radical anion coupling) if the potential is extended only to the first reduction process. However, the reverse oxidation process (III_{ox}) that is observed when the potential is extended past the second one-electron transfer to form the dianion may not be associated with just dimer formation.

3.2. Cyclic Voltammetry of Retinal in Acetonitrile with Variable Water Concentrations. Previous studies have indicated that water plays a role in the reduction mechanism of retinal in organic solvents,^{23,24} thus, it is important to quantitatively determine exactly how water affects the electrochemical behavior of the starting material and the electrochemically generated species.³⁹ Water is an ever-present impurity in organic solvents and normally exists in a substantially higher concentration than the analyte, unless scrupulous care is taken to remove it.³¹ Electrochemical reactions involving the accurate addition of water are difficult to perform because of natural contamination from the atmosphere into the electrochemical cell over time. Although an initial water content of 20 mM can be achieved in the electrochemical cell at room temperature, the value quickly increases, especially at lower temperatures.

With a water content of 20 mM, it was observed that peaks I_{ox} and III_{ox} were a similar size at a scan rate of 0.1 V s^{-1} (Figure 6). This was not the same as the voltammogram obtained with a higher water content (Figure 5) in which III_{ox} appears larger than I_{ox} at the same scan rate and retinal concentration. This result indicates that the species responsible for III_{ox} is both a dimeric compound (formed by dimerization of the radical anion) and a reaction product that is favored in the presence of water.

When water was progressively added to the solvent and voltammograms were conducted over a range sufficiently negative to form only the anion radical (Figure 6b), oxidation process III_{ox} became relatively larger compared to oxidation process I_{ox} , suggesting that oxidation process III_{ox} is partly associated with a reaction product of $\text{R}^{\bullet-}$ (in addition to a dimeric species). Similarly, when the forward potential scan was extended so as to form the dianion (Figure 6a), process III_{ox} became much larger as more water was added to the solvent (up to 1 M), suggesting that the dianion undergoes a decomposition reaction and that this occurs to a greater extent than for the anion radical (by a comparison of Figure 6a,b). At very high water concentrations ($>0.5 \text{ M}$), process III_{ox} substantially decreases in size and takes on a more complicated shape, possibly because of competing hydrolysis reactions making new compounds that are oxidized at different potentials.

It was also noticed that the second reduction peak changes in shape as more water is added to the solution, becoming progressively flatter. The peak potential shifts to more positive potentials as water is added, making it easier to reduce the starting material and radical anion. The shift in potential can be attributed to a hydrogen-bonding mechanism that is often observed during the reduction of quinones, where the hydrogen bonding facilitates the reduction processes.^{40–42} Although it could be argued that process III_{ox} is actually associated simply with the oxidation of a hydrolyzed product of the anion radical

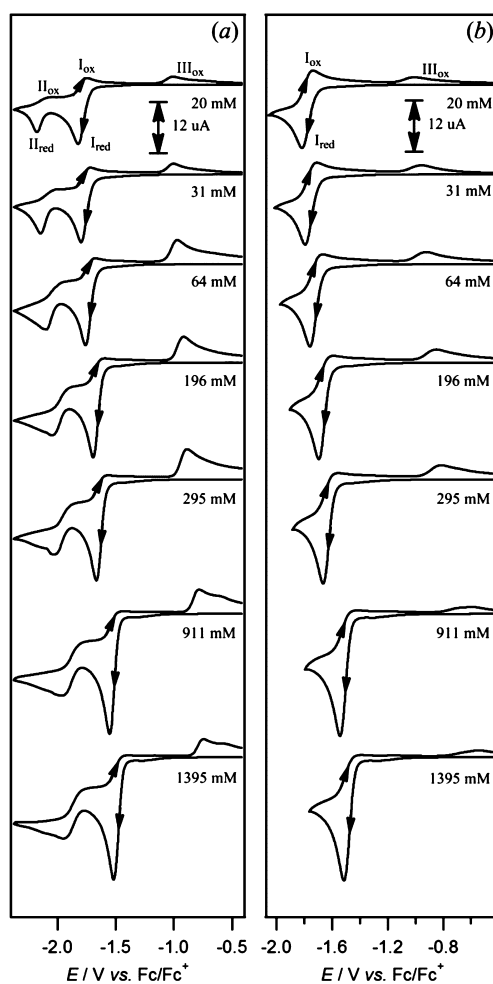


Figure 6. CV data of $5 \times 10^{-3} \text{ M}$ retinal in CH_3CN containing 0.2 M Bu_4NPF_6 at $295 \pm 2 \text{ K}$ obtained at a 1 mm GC working electrode at a scan rate of 0.1 V s^{-1} with varying amounts of water.

and dianion (or a product favored in the presence of water), this is not consistent the fact that process III_{ox} becomes larger (relative to process I_{ox}) when the concentration of retinal is increased (Figure 5). As the concentration of retinal increases, there are actually fewer water molecules per molecule of retinal; thus, it would be expected that a reaction product that is favored in the presence of water would result in process III_{ox} becoming relatively smaller compared to process I_{ox} , which is the opposite of what is observed. Therefore, it is proposed that process III_{ox} is associated with oxidation of both a dimeric compound ($\text{R}_2^{\bullet-}$) that forms via dimerization of $\text{R}^{\bullet-}$ as well as a decomposition product X formed from R^{2-} that is favored in the presence of H_2O .

3.3. Digital Simulation of CV Measurements on Retinal with Variable Water Concentrations and Temperature. Digital simulation studies were performed to determine the most appropriate mechanism to account for the voltammetric behavior of retinal. The simulations were performed by a trial and error process that involved systematically expanding the steps in the electrochemical mechanism using one set of parameters over all scan rates (for each individual temperature) until the simulated voltammograms matched the experimental voltammograms. Initially, the diffusion coefficient (D) of retinal was determined from the reductive peak current of the first process, while the D

Table 1. Equilibrium and Rate Constants Obtained by Digital Simulation of CV Data for the Reaction Mechanism Given in Scheme 2^a

temperature(K)	kinetic parameters	Eq 1	Eq 2	Eq 3	Eq 4	Eq 5	Eq 6
295 ± 2 (dry)	K_{eq}	5×10^4	1×10^7	1×10^3	1×10^4	5×10^4	3×10^4
	k_f	2×10^1	3×10^2	1×10^2	1×10^2	5×10^3	5×10^2
	k_b	4×10^{-4}	3×10^{-5}	1×10^{-1}	1×10^{-2}	1×10^{-1}	2×10^{-2}
295 ± 2	K_{eq}	2×10^4	2×10^5	3×10^3	8×10^3	5×10^4	4×10^4
	k_f	2×10^0	1×10^2	3×10^2	5×10^2	5×10^3	8×10^2
	k_b	1×10^{-4}	5×10^{-4}	1×10^{-1}	6×10^{-2}	1×10^{-1}	2×10^{-2}
273	K_{eq}	1×10^4	2×10^5	5×10^3	5×10^3	1×10^5	5×10^5
	k_f	2×10^0	1×10^2	3×10^2	5×10^2	1×10^3	1×10^3
	k_b	2×10^{-4}	5×10^{-4}	6×10^{-2}	1×10^{-1}	5×10^{-2}	2×10^{-3}
253	K_{eq}	5×10^3	2×10^5	8×10^3	1×10^3	2×10^5	1×10^6
	k_f	2×10^0	1×10^2	5×10^2	1×10^2	2×10^3	6×10^2
	k_b	4×10^{-4}	5×10^{-4}	6×10^{-2}	1×10^{-1}	1×10^{-2}	6×10^{-4}

^aCV data recorded in CH₃CN with 0.2 M *n*-Bu₄NPF₆ at a 1 mm diameter GC electrode at scan rates of 0.1–20 V s⁻¹ and at water concentrations between 0.020 and 0.1 M, where 0.020 was used for the dry conditions and 0.05–0.1 M for noncontrolled conditions. Heterogeneous rate constants were estimated to be 0.5 cm s⁻¹. Diffusion coefficient values for retinal were 1.25×10^{-5} cm² s⁻¹ at 295 K, 9.00×10^{-6} cm² s⁻¹ at 273 K, and 6.00×10^{-6} cm² s⁻¹ at 253 K. The diffusion coefficient value for water was set at 1.00×10^{-5} cm² s⁻¹. Homogeneous rate constants for the forward (k_f) and backward (k_b) reactions have units of s⁻¹ and L mol⁻¹ s⁻¹ for the first- and second-order reactions, respectively.

obtained for the EC_{dim} mechanism, which was modeled to involve both the H-bonded and non H-bonded radical anions. The simulations indicate that the equilibrium constants for the dimerization reactions (Eq 5 and Eq 6 in Scheme 2) increase as the temperature decreases, which is similar to the results obtained from other electrochemical studies on reversible dimerization reactions indicating that the dimerization is favored at lower temperatures.^{32–38}

Although Figure 7 shows that the simulations could be made to closely fit the experimental data, the large number of parameters used in the simulations means that the values given in Table 1 are not necessarily a unique set. A further complication is that many of the parameters are interrelated in such a way that varying one necessitates altering the others to maintain the close fit. Nevertheless, it was found that in all instances the degree of variation (and the estimated error) was substantially less than 1 order of magnitude, which is a reasonable degree of precision considering the large number of steps in the mechanism.

A set of “dry” experimental results were also simulated to fit the measured water content of 20 mM at room temperature while normal nonwater controlled conditions used a water concentration of 50 (±10) mM.

The simulations indicated that the potential of the first reduction process ($E^{\circ}_{(1)}$) occurred at -1.75 (±0.04) V vs Fc/Fc⁺ while the second reduction process ($E^{\circ}_{(2)}$) occurred at -2.15 (±0.04) V vs Fc/Fc⁺. The reduction potential ($E^{\circ}_{(3)}$) of the strongly hydrogen-bonded (with water) radical anion occurred at a slightly more positive potential of -2.05 (±0.02) V vs Fc/Fc⁺. Process III_{ox} consists of multiple species undergoing oxidation ($E^{\circ}_{(4,5)}$) at slightly varying potentials ranging from -0.83 V vs Fc/Fc⁺ to -1.08 V vs Fc/Fc⁺. Oxidation of the dimer dianion that is formed from two molecules of the anion radical takes place at a potential that is slightly more positive than that of the oxidation of product X that is formed via a decomposition reaction of the dianion. The assignment of peak III_{ox} as consisting of at least two processes was deduced by comparing the voltammograms obtained with different switching potentials. The oxidation process (III_{ox}) that was detected when the scan direction was reversed just after I_{red} occurred at a potential that was more positive than that of the

oxidation process detected when the scan direction was reversed after II_{red}. Furthermore, it was found that when water was progressively introduced into the solution, the reduction peak potentials shifted to more positive potentials, which is likely due to hydrogen-bonding interactions.^{39–42}

4. CONCLUSIONS

The results of this study indicate that retinal undergoes a series of homogeneous reactions following heterogeneous electron transfer that critically depend on retinal concentration, temperature, and water content of the acetonitrile solutions. At low water concentrations, low temperature, and high retinal concentrations, dimerization of the anion radical is the favored reaction mechanism. As the water content increases, hydrolysis reactions (including hydrogen bonding) and decomposition of the dianion of retinal dominate. The electrochemical mechanism was particularly difficult to study because both major products of the reduction (dimer dianions and decomposition products) were themselves oxidized at very similar potentials, comprising oxidation process III_{ox}.

The experimental apparatus used for electrochemical experiments makes it difficult to completely exclude water from electrochemical cells. Furthermore, the requirement that voltammetric experiments be performed at relatively low analyte concentrations (<10 mM) to avoid deleterious effects in modeling the data (such as IR drop and migration), means that in most circumstances there will be more water than substrate. Therefore, the full interpretation of the voltammetric behavior of retinal requires knowledge of the water content of the solution. Whether these reactions occur biologically remains to be determined, but it is interesting that even relatively small amounts of water can substantially alter the reduction mechanism. Furthermore, it is also likely that other hydrogen-bonding donors such as amines, which are present in lipophilic membrane environments, will also affect the electrochemical behavior of retinal.

■ AUTHOR INFORMATION

Corresponding Author

*Email: webster@ntu.edu.sg. Tel: +65 6316 8793.

Notes

The authors declare no competing financial interest.

ACKNOWLEDGMENTS

This work was supported by an A*Star SERC Public Sector Funding (PSF) Grant (112 120 2006).

REFERENCES

- (1) McMurry, J. E.; Fleming, M. P. A New Method for the Reductive Coupling of Carbonyls to Olefins. Synthesis of β -Carotene. *J. Am. Chem. Soc.* **1974**, *96*, 4708–4709.
- (2) Nagao, A. Oxidative Conversion of Carotenoids of Retinoids and Other Products. *J. Nutr.* **2004**, *134*, 237S–240S.
- (3) Ziyatdinova, G.; Giniyatova, E.; Budnikov, H. Cyclic Voltammetry of Retinol in Surfactant Media and Its Application for the Analysis of Real Samples. *Electroanalysis* **2010**, *22*, 2708–2713.
- (4) Krinsky, N. I.; Yeum, K. -J. Carotenoid-Radical Interactions. *Biochem. Biophys. Res. Commun.* **2003**, *305*, 754–760.
- (5) Loessing, I. T. *Vitamin A: New Research*; Nova Biomedical Books: New York, 2007; pp 39–57.
- (6) Ball, G. F. M. *Vitamins: Their Role in the Human Body*, 1st ed.; Blackwell Publishing Ltd.: Ames, IA, 2004.
- (7) Webster, R. D. Voltammetry of the Liposoluble Vitamins (A, D, E and K) in Organic Solvents. *Chem. Rec.* **2012**, *12*, 188–200.
- (8) Suarez-Fernandez, A. L.; Alarnes-Varela, G.; Costa-Garcia, A. Electrode Kinetic Studies of β -Carotene in Aprotic Solvents with Carbon Fiber Microelectrodes. *Electrochim. Acta* **1999**, *44*, 4489–4498.
- (9) Lehninger, A. L.; Nelson, D. L.; Cox, M. M. *Principles of Biochemistry*; W. H. Freeman: New York, 2000.
- (10) Murray, R. K.; Granner, D. K.; Mayes, P. A.; Rodwell, V. W. *Harper's Illustrated Biochemistry*, 26th ed.; McGraw-Hill Medical: New York, 2003.
- (11) Mairanovsky, V. G.; Engovatov, A. A.; Ioffe, N. T.; Samokhvalov, G. I. Electron-Donor and Electron-Acceptor Properties of Carotenoids: Electrochemical Study of Carotenes. *J. Electroanal. Chem.* **1975**, *66*, 123–137.
- (12) Burton, G. W.; Ingold, K. U. β -Carotene: An Unusual Type of Lipid Antioxidant. *Science* **1984**, *224*, 569–573.
- (13) Park, S.-M. Electrochemical Studies of β -Carotene, all-*trans*-Retinal and all-*trans*-Retinol in Tetrahydrofuran. *J. Electrochem. Soc.* **1978**, *125*, 216–222.
- (14) Lang, C. M.; Harbour, J.; Guzzo, A. V. The Radical Anions of Vitamin A Aldehyde and Related Schiff Bases. *J. Phys. Chem.* **1971**, *75*, 2861–2866.
- (15) Powell, L. A.; Wightman, R. M. Spectroelectrochemistry of Retinal. Electrodimerization in the Presence of Proton Donors. *J. Electroanal. Chem.* **1980**, *106*, 377–390.
- (16) Nelson, A. Voltammetry of Retinal in Phospholipid Monolayers Adsorbed on Mercury. *J. Electroanal. Chem.* **1992**, *335*, 327–343.
- (17) Costentin, C.; Savéant, J. M. Dimerization of Electrochemically Generated Ion Radicals: Mechanisms and Reactivity Factors. *J. Electroanal. Chem.* **2004**, *564*, 99–113.
- (18) Sioda, R. E.; Terem, B.; Utley, J. H. P.; Weedon, B. C. L. Electro-organic Reactions. Part V. Cathodic Pinacolisation of α and β -ionones. *J. Chem. Soc., Perkin Trans. 1* **1976**, 561–563.
- (19) Sopher, D. W.; Utley, J. H. P. Electrochemical Pinacolisations Modified by Chromium (III). *J. Chem. Soc., Chem. Commun.* **1979**, 1087–1088.
- (20) Lamy, E.; Nadjo, L.; Savéant, J. M. Electrodimerization X. Solvation and Protonation in the EHD [Electrohydrodimerization] of Activated Olefins in Low Acidity Media. *J. Electroanal. Chem.* **1974**, *50*, 141–145.
- (21) Savéant, J. M.; Tessier, D. Non-Volmerian Charge Transfers Associated with Follow-Up Chemical Reactions. A Convolution Potential Sweep Voltammetric Study of Benzaldehyde Reduction in Ethanol. *J. Phys. Chem.* **1978**, *82*, 1723–1727.
- (22) Andrieux, C. P.; Grzeszczuk, M.; Savéant, J. M. Electrochemical Generation and Reduction of Organic Free Radicals. α -Hydroxybenzyl Radicals from the Reduction of Benzaldehyde. *J. Am. Chem. Soc.* **1991**, *113*, 8811–8817.
- (23) Powell, L. A.; Wightman, R. M. Electroreduction of Retinal. Formation of Pinacol in the Presence of Malonate Esters. *J. Am. Chem. Soc.* **1979**, *101*, 4412–4413.
- (24) Powell, L. A.; Wightman, R. M. Mechanism of Electrodimerization of Retinal and Cinnamaldehyde. *J. Electroanal. Chem.* **1981**, *117*, 321–333.
- (25) Rudolph, M. Digital Simulations on Unequally Spaced Grids. Part 2. Using the Box Method by Discretisation on a Transformed Equally Spaced Grid. *J. Electroanal. Chem.* **2003**, *543*, 23–39.
- (26) Rudolph, M. Reply to L. K. Bieniasz's Comments on my Paper [J. Electroanal. Chem. 529 (2002) 97]. *J. Electroanal. Chem.* **2003**, *558*, 171–176.
- (27) Rudolph, M. Digital Simulations on Unequally Spaced Grids. Part 3. Attaining Exponential Convergence for the Discretisation Error of the Flux as a New Strategy in Digital Simulations of Electrochemical Experiments. *J. Electroanal. Chem.* **2004**, *571*, 289–307.
- (28) Rudolph, M. Attaining Exponential Convergence for the Flux Error with Second- and Fourth-Order Accurate Finite-Difference Equations. I. Presentation of the Basic Concept and Application to a Pure Diffusion System. *J. Comput. Chem.* **2005**, *26*, 619–632.
- (29) Rudolph, M. Attaining Exponential Convergence for the Flux Error with Second- and Fourth-Order Accurate Finite-Difference Equations. II. Application to Systems Comprising First-Order Chemical Reactions. *J. Comput. Chem.* **2005**, *26*, 633–641.
- (30) Rudolph, M. Attaining Exponential Convergence for the Flux Error with Second- and Fourth-Order Accurate Finite-Difference Equations. Part 3. Application to Electrochemical Systems Comprising Second-Order Chemical Reactions. *J. Comput. Chem.* **2005**, *26*, 1193–1204.
- (31) Hui, Y.; Webster, R. D. Absorption of Water into Organic Solvents Used for Electrochemistry under Conventional Operating Conditions. *Anal. Chem.* **2011**, *83*, 976–981.
- (32) Hammerich, O.; Parker, V. D. Kinetics and Mechanisms of Reactions of Organic Cation Radicals in Solution. *Adv. Phys. Org. Chem.* **1984**, *20*, 55–189.
- (33) Amatore, C.; Garreau, D.; Hammi, M.; Pinson, J.; Savéant, J. M. Kinetic Analysis of Reversible Electrodimerization Reactions by the Combined use of Double Potential Step Chronoamperometry and Linear Sweep Voltammetry. Application to the Reduction of 9-Cyanoanthracene. *J. Electroanal. Chem. Interfacial Electrochem.* **1985**, *184*, 1–24.
- (34) Webster, R. D. EPR and Voltammetric Evidence for the Reversible Dimerization of Anion Radicals of Aromatic Meta-Substituted Diesters and Dithioic S,S'-Diesters. *J. Chem. Soc., Perkin Trans. 2* **1999**, 263–270.
- (35) Mazine, V.; Heinze, J. Dimerization of Electrochemically Generated Radical Ions under High Pressure. *J. Phys. Chem. A* **2004**, *108*, 230–235.
- (36) Macías-Ruvalcaba, N. A.; Felton, G. A. N.; Evans, D. H. Contrasting Behavior in the Reduction of 1,2-Acenaphthylenedione and 1,2-Aceanthrylenedione. Two Types of Reversible Dimerization of Anion Radicals. *J. Phys. Chem. C* **2009**, *113*, 338–345.
- (37) Macías-Ruvalcaba, N. A.; Evans, D. H. Association Reactions of the Anion Radicals of Some Hydroxyquinones: Evidence for Formation of π - and σ -Dimers As Well As a Neutral–Anion Radical Complex. *J. Phys. Chem. C* **2010**, *114*, 1285–1292.
- (38) Haubner, K.; Tarábek, J.; Ziegs, F.; Lukeš, V.; Jaehne, E.; Dunsch, L. Charged States of α,ω -Dicyano β,β' -Dibutylquaterthiophene as Studied by in Situ ESR UV–Vis NIR Spectroelectrochemistry. *J. Phys. Chem. A* **2010**, *114*, 11545–11551.
- (39) Tan, Y. S.; Chen, S.; Hong, W. M.; Kan, J. M.; Kwok, E. S. H.; Lim, S. Y.; Lim, Z. H.; Tessensohn, M. E.; Zhang, Y.; Webster, R. D. The Role of Low Levels of Water in the Electrochemical Oxidation of α -Tocopherol (Vitamin E) and Other Phenols in Acetonitrile. *Phys. Chem. Chem. Phys.* **2011**, *13*, 12745–12754.

(40) Gupta, N.; Linschitz, H. Hydrogen-Bonding and Protonation Effects in Electrochemistry of Quinones in Aprotic Solvents. *J. Am. Chem. Soc.* **1997**, *119*, 6384–6391.

(41) Quan, M.; Sanchez, D.; Wasylkiw, M. F.; Smith, D. K. Voltammetry of Quinones in Unbuffered Aqueous Solution: Reassessing the Roles of Proton Transfer and Hydrogen Bonding in the Aqueous Electrochemistry of Quinones. *J. Am. Chem. Soc.* **2007**, *129*, 12847–12856.

(42) Hui, Y.; Chng, E. L. K.; Chng, C. Y. L.; Poh, H. L.; Webster, R. D. Hydrogen-Bonding Interactions Between Water and the One- and Two-Electron-Reduced Forms of Vitamin K₁: Applying Quinone Electrochemistry To Determine the Moisture Content of Non-Aqueous Solvents. *J. Am. Chem. Soc.* **2009**, *131*, 1523–1534.

(43) Bauer, P. -J.; Carl, P. Dielectric Studies on Retinal and Ionone. *J. Am. Chem. Soc.* **1977**, *99*, 6850–6855.